MRI of the Fetal Chest

9

Dorothy Bulas and Alexia Egloff

9.1 Introduction

A wide variety of chest abnormalities can be identified prenatally. The natural history and prognosis are variable depending on the type and size of the abnormality. Some lesions can be asymptomatic with a favorable prognosis; others can result in significant fetal and/or neonatal distress requiring fetal intervention. Thorough examination is needed to provide an accurate diagnosis and help determine adequate pre- and postnatal management. Ultrasound is the screening method of choice in the evaluation of the fetus and successful diagnoses of many fetal thoracic abnormalities. MRI has been increasingly used as an adjunct examination, for central nervous system abnormalities, but is also beneficial in the evaluation of extracranial abnormalities [1, 2]. Several studies demonstrate that additional useful information in the evaluation of the fetal chest can be obtained with MRI, even after a diagnosis has been made by ultrasound (38–50 % additional information) [1, 3, 4]. At times, MRI can provide information that changes pre- and postnatal management. At other times, the MRI may simply confirm the diagnosis, increasing confidence of management planning and appropriate patient counseling [3, 5].

Several advantages are seen when using MRI in the assessment of lung anomalies compared to ultrasound, including its multiplanar capability, large field of view, and soft tissue contrast between the bowel, liver, normal lung, and lung masses. The large field of view allows improved visualization of the lesions, useful for families and specialists to review and understand. In the setting of oligohydramnios and maternal obesity, MRI can delineate structures when US is unable to. MRI is not operator dependent, a vulnerability of ultrasound. Improvements in ultrafast sequences help reduce motion artifact and have diminished the need for sedation.

Volume measurements can be reliably obtained. Research using different MR imaging sequences has shown an increase in lung apparent diffusion coefficient with increase in gestational age and may represent an increase in vascularity [6].

Spectroscopy has the potential of estimating the amount of choline-containing compounds and could be useful in the assessment of lung maturation as well [7]. These other MR imaging techniques need further research to demonstrate their importance.

9.2 Technique and Normal Appearance

Different MRI sequences are needed to fully evaluate the fetal chest, including single-shot fast spin echo (SSFSE), steady-state free precession (SSFP), and gradient echo (GRE) sequences, and should be obtained in all three planes. Different structures within the thorax are better seen in certain planes of imaging.

Coronal, axial, and sagittal SSFSE allow visualization of the lungs. Axial, long-, and short-axis SSFP can help evaluate the great vessels and heart. The thymus is best seen on axial and coronal SSFSE and the diaphragm in coronal and sagittal SSFSE. Dynamic SSFP can document cardiac and diaphragmatic motion as well as swallowing. When congenital diaphragmatic hernia is suspected, SSFSE in all three planes helps lung volume determination. Coronal and sagittal T1-weighted GRE is helpful in assessing the location of the liver and meconium-filled loops of the bowel.

D. Bulas, MD (✉)
Department of Diagnostic Imaging and Radiology,
Children's National Medical Center,
111 Michigan Ave NW, Washington, DC 20010, USA
e-mail: DBULAS@childrensnational.org

A. Egloff, MD
Department of Diagnostic Imaging and Radiology,
Children's National Medical Center,
Washington, DC 20010, USA

G. Masselli (ed.), *MRI of Fetal and Maternal Diseases in Pregnancy*, DOI 10.1007/978-3-319-21428-3_9

Fig. 9.1 (**a**) Coronal SSFSE T2w image of a fetal chest at 24 weeks gestation with intermediate signal lung parenchyma. Note the fluid-filled trachea and bronchi (**b**). Coronal SSFSE T2w image of a fetal chest at 35 weeks gestation. Note the increase in signal of the parenchyma as compared to 24 weeks GA

Lung parenchyma is homogeneously brighter than the muscle on T2w images and increases in signal after 24 weeks of gestation (Fig. 9.1), while T1w signal decreases with gestational age. Fetal lungs increase in volume throughout gestation and can be measured with MRI volumetry. Normal lung volumes demonstrate proportionate growth to fetal body size.

The airways, including the trachea, carina, and bronchi, are typically filled with fluid and thus appear bright on T2w (Fig. 9.1a). When needed, repeating sequences with thinner slices may be beneficial for further evaluation.

The thymus is a homogeneous anterior mediastinal structure which should not exert any mass effect on surrounding structures. It is homogeneously intermediate in signal best seen in the third trimester as it increases in size.

The heart is low signal on T2w SSFSE due to flowing blood. SSFP sequences are more useful in delineating the myocardium, septum, and valves (Fig. 9.2). Dynamic SSFP sequences can demonstrate cardiac motion.

The diaphragms are dome-shaped bands between the lungs and the abdomen. They have low signal on T2w, slightly lower than the adjacent liver. Breathing may be noted on dynamic SSFP sequences.

9.3 Lung Development

Different but overlapping stages of maturation are seen in the lungs throughout gestation. Stages include embryonic (26 days to 6 weeks), pseudoglandular (6–16 weeks), canalicular (16–28 weeks), saccular (28–36 weeks), and alveolar (36 weeks to childhood). There is an overlap between these stages due to differing speeds of maturation between central and peripheral lung regions and cephalad and caudal segments [8, 9].

During the embryonic stage, the laryngotracheal tube originates as a ventral diverticulum from the primitive

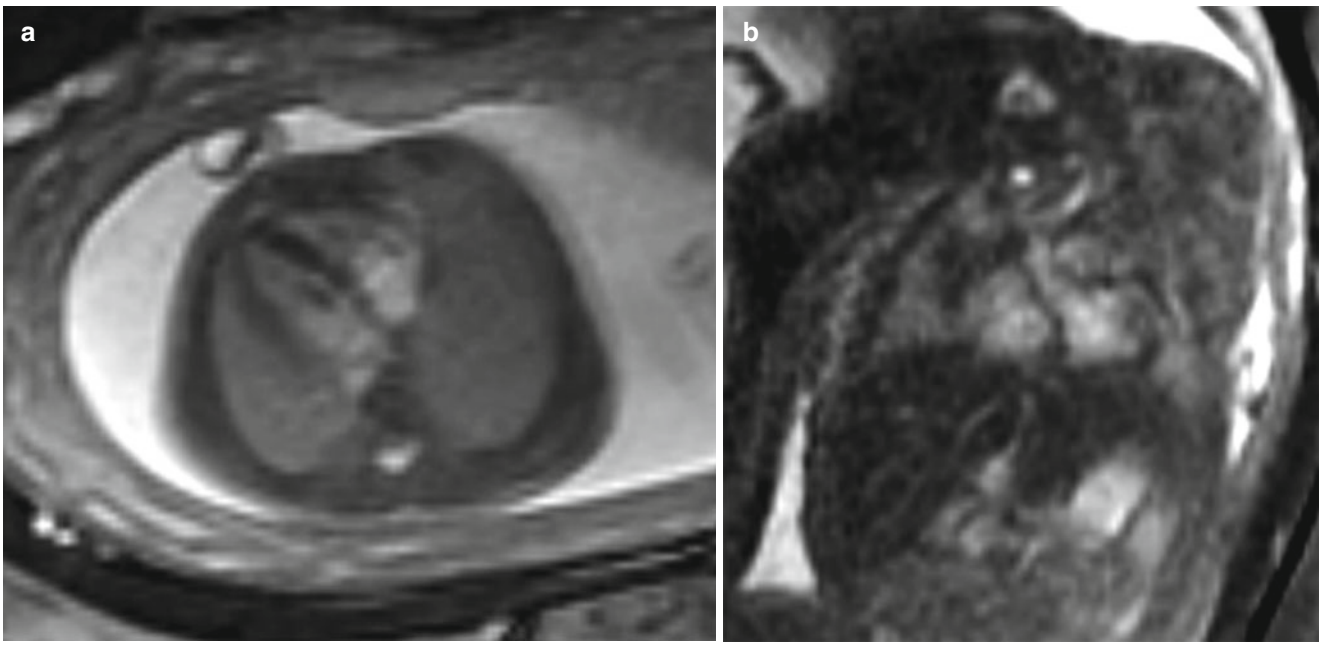

Fig. 9.2 (**a**) Axial SSFP image at 27 weeks gestation demonstrates normal axis of the four-chamber view of the heart. The blood is bright on this sequence allowing visualization of the ventricular septum. (**b**) Coronal SSFP image demonstrates the left ventricular outflow track

pharynx. With time, it elongates to form the larynx and trachea from its proximal end and the lung buds distally.

By days 26–28, the lung buds enlarge and divide. A right and left bud will continue to branch during the fifth week of gestation, forming three secondary branches on the right and two on the left. Further dichotomous branching continues to occur until the 20th week when the terminal bronchioles are formed. Several more divisions occur to form the respiratory bronchioles. Major structures are formed by 28th week but the lungs continue to mature until early childhood.

The diaphragm has four different embryonic origins: the septum transversum, the pleuroperitoneal membranes, the paraxial mesoderm of the body wall, and the esophageal mesenchyme.

9.4 Abnormalities of the Fetal Thorax

9.4.1 Congenital Diaphragmatic Hernia (CDH)

9.4.1.1 Definition

CDH is a congenital anomaly that affects the development of the diaphragm and allows for intra-abdominal organs to move into the thoracic cavity. It results in lung hypoplasia from lung compression and mechanical complications from mediastinal and cardiac deviation.

9.4.1.2 Classification

CDH can be classified based on location: posterolateral Bochdalek hernia (70–75 %), anterior Morgagni hernia (23–28 %), and central defects (2–7 %) [10]. Most CDHs occur on the left side (85–90 %), some on the right (10–15 %), and only rarely bilaterally (2 %) [11].

CDH can also be differentiated as isolated or complex. CDH is often isolated. However, in 23–43 % of cases, an associated anomaly can be present [12], most likely a cardiac defect (20 %) [11, 13, 14]. When multiple abnormalities are present, genetic anomalies should be considered with a higher mortality [14]. More than 50 genetic causes have been described and can vary from chromosomal abnormalities such as trisomy 18, microdeletions, or microduplications to syndromes with unknown genetic mutations (Fryns syndrome).

9.4.1.3 Imaging Findings

US findings seen in patients with CDH include presence of stomach bubble, gallbladder or bowel within the thoracic cavity, deviation of the heart and mediastinum, herniated liver, abnormal position of the umbilical and hepatic veins, pleural effusion, and polyhydramnios [11, 13, 15]. MRI is an adjuvant study helping to confirm the diagnosis, aiding in the search for additional abnormalities, and providing additional data such as lung volumes that may help predict outcome.

MRI better demonstrates the position of the liver and the amount of herniation due to superior differentiation of the hepatic lobe (bright on T1) from the compressed lung or a

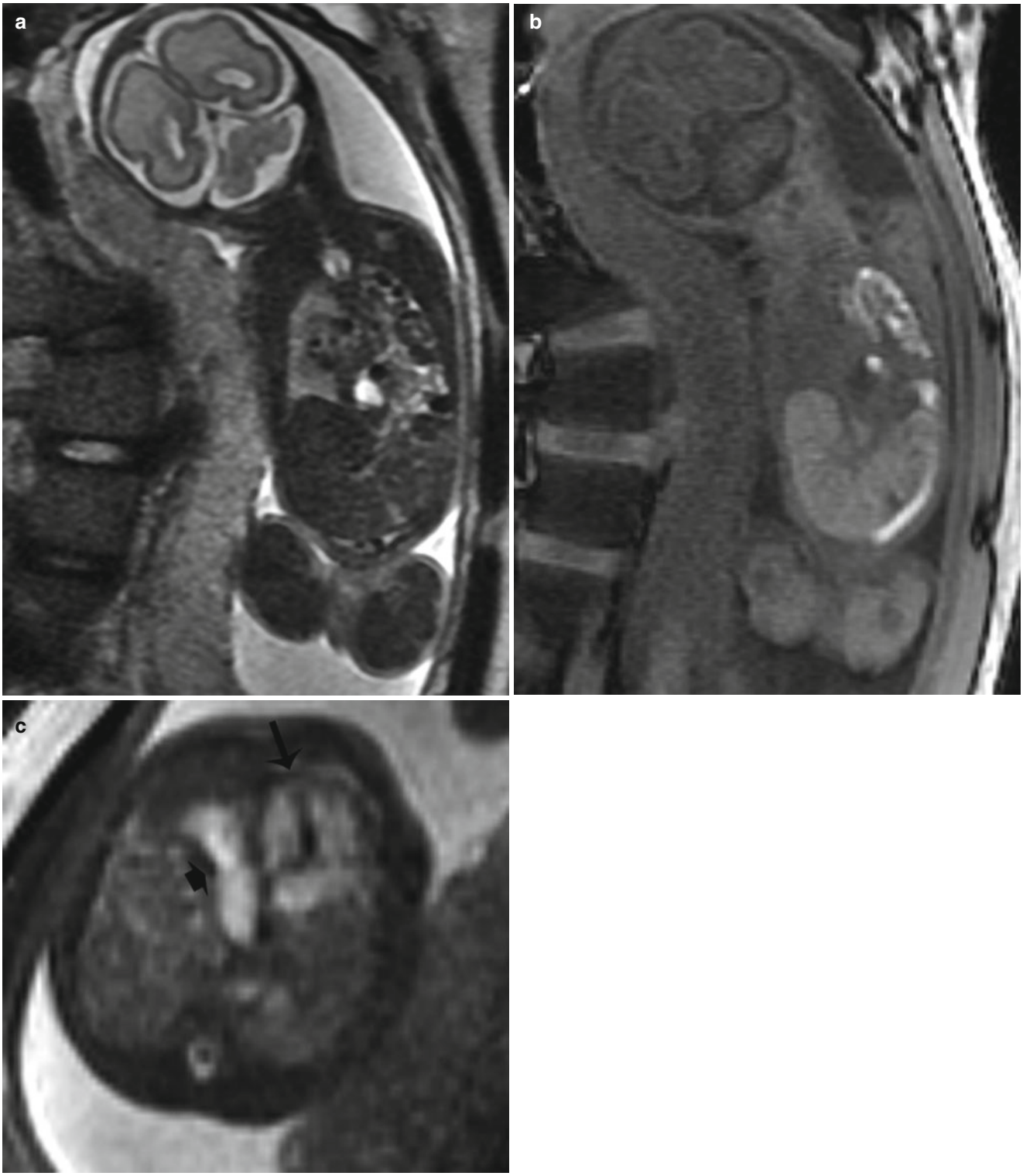

Fig. 9.3 Left CDH at 26 weeks gestation. (**a**) Coronal SSFSE image demonstrates bowel filling of the left hemithorax. Residual lung is noted on the right. (**b**) Coronal T1w image demonstrates meconium-filled bowel herniated into the left hemithorax. (**c**) Axial SSFP image of the chest demonstrate the heart (*long arrow*) to be shifted moderately to the right. The stomach (*short arrow*) is herniated into the chest with heterogenous collapsed bowel posterior to the stomach. A small amount of herniated left lobe of the liver is noted anterior to the stomach

solid type of CPAM [16–18]. MRI can also help by providing better evaluation of the bowel with bright T1 signal of meconium and allowing visualization of the normal ipsilateral and contralateral lung [19] which is useful in the assessment of pulmonary hypoplasia [7] (Fig. 9.3). Suggestion of a hernia sac by a rounded appearance of the

Fig. 9.4 Membrane-covered CDH at 22 weeks gestation. (**a**) Coronal SSFSE image demonstrates elevated left hemidiaphragm with residual left upper lung. (**b**) Coronal T1w image demonstrates herniation of the liver into the left hemithorax. The infant did well after delivery without requiring ECMO

most superior aspect of the hernia has been associated with a better prognosis [7, 16] (Fig. 9.4).

Different volumetric measurements can be obtained with MRI and used as indicators of outcome. MR measurements allow assessment of both lungs and can be more reliably obtained than US [17]. MRI measurements include total lung volume, observed to expected total lung volume (o/e TLV), percent predicted lung volume (PPLV), fetal lung volume to fetal body volume ratio (FLV/FBV), percent liver herniation (%LH), and herniated liver to fetal thoracic volume ratio (LiTR).

MRI can measure the diameter of the aorta and pulmonary arteries used to obtain the modified McGoon index as a prognostic indicator of pulmonary hypertension [19].

Imaging with diffusion-weighted sequences to assess growth and maturity has been attempted though no correlation has been seen with lung volume or fetal survival [20].

9.4.1.4 Prognosis and Fetal Management

Prognosis varies depending on the side of the herniation, the position of the liver, associated abnormalities, and age at diagnosis [12].

The presence of herniated liver decreases survival from 74 to 45 % [21], and the presence of associated anomalies also decreases the survival [12]. The severity of lung hypoplasia and resulting lung hypertension are major determinants in the mortality and morbidity of the patients [22–24], and a larger herniation diagnosed earlier results in worse pulmonary hypoplasia with a resulting higher mortality.

Bilateral hernias are usually fatal. Familial and syndromic hernias usually have a worse prognosis compared to isolated hernias [25].

Different ultrasound and MRI measurements have been used to estimate the severity of lung hypoplasia and probable outcome of the fetus:

(a) Lung to head circumference ratio (LHR), obtained by ultrasound, has been used as a predictor of outcome and as indicator of the need of more aggressive treatment such as ECMO. LHR less than 1 is seen in patients with poor outcome, with a survival rate of 45 % [15, 26]. LHR's prognostic value is variable due to differences

in methodology, compression of normal lung, and dependence on gestational age [25], resulting in a controversial association with mortality [22].

(b) Observed to expected lung head ratio (o/e LHR) was developed as an ultrasound measurement [27–29] with better predictive value over LHR [25, 30]. A ratio of 25 % or less suggests lower survival rates [28].

(c) Total lung volumes have been used to quantify degree of lung hypoplasia. A better prognosis is expected in fetuses with a total lung volume of 25 cm^3 or more, compared to fetuses with a lung volume of 18 cm^3 or less.

(d) o/e TLV has a good correlation with ultrasound obtained LHR and has better predictive value compared to total lung volumes but is operator dependent and affected by motion [30]. Mortality rate of 87 % was seen in fetuses with o/e TLV of less than 25 %, and it decreased to 31 % in those fetuses with an o/e TLV of 25–35 % and further decreased to 17 % in those with an o/e TLV of more than 35 % [25].

(e) Percent predicted lung volume (PPLV) is obtained by dividing the volume of the CDH by the volume of the expected lung volume; the expected lung volume is obtained by measuring the total lung volume and subtracting the mediastinal volume [31]. If PPLV is greater than 15 %, a good outcome with 100 % survival can be expected; if PPLV is less than 15 %, bad outcome is likely, with only 40 % survival [31].

(f) %LH is the ratio obtained between the herniated liver and the total volume of the liver. It shows an accuracy of 87 % in predicting mortality [32].

(g) LiTR is the ratio of herniated liver volume to total thoracic volume without the spine and has 85 % accuracy in predicting mortality [33].

(h) FLV/FBV ratio. This measurement is equivalent to the postmortem lung weight to body weight ratio used to evaluate pulmonary hypoplasia. A lower ratio is associated with increased mortality [34].

In a study by Ruano et al., the best combination of measurements to assess mortality is o/e TLV and %LH [24].

Ultrasound methods exist to predict pulmonary hypertension. By MRI, the modified McGoon index can be obtained by adding the right pulmonary artery diameter plus left pulmonary artery diameter and dividing the sum by the diameter of the descending aorta measured at the level of the diaphragm [19].

Complete anatomical examination should be performed to assess for presence of associated anomalies (25–75 %) [35]. Echocardiography is indicated as congenital cardiac defects occur in 10–35 % of cases and decrease survival from 73 to 67 % if it is a minor defect or 36 % if major complex cardiac defect [25].

A prenatal karyotype with microarray is indicated to assess for chromosomal anomalies, present in 10–20 % of cases [14, 35].

Follow-up ultrasound examinations should be performed to assess fetal well-being, lung volume, and changes in mediastinal shift that could result in hemodynamic changes [36]. Third trimester follow-up MRI can be performed to assess lung volume near time of maximal intrauterine growth and plan delivery; this late MRI can also be used for postnatal surgical planning decreasing the need for postnatal cross-sectional imaging [19].

Different fetal surgical techniques have been attempted, such as in utero repair and fetal tracheal occlusion via open surgery or endoscopy, with clip or balloon occlusion. EXIT to ECMO is also offered in some centers but has not demonstrated significant survival benefits [21]. New nonsurgical prenatal options are being evaluated, including pharmacologic treatments and stem-cell-based strategies, and could be promising in treating pulmonary hypertension and hypoplasia [23].

9.4.2 Congenital Pulmonary Airway Malformation (CPAM)

9.4.2.1 Definition

CPAM is a congenital anomaly of the lung resulting in a cystic, hamartomatous mass of lung tissue that communicates with the bronchial tree through an abnormal communication and has normal pulmonary blood supply and venous drainage into the normal pulmonary veins [37].

9.4.2.2 Classification

CPAM has been classically classified based on pathology by Stocker et al. into type I (large cysts, more than 2 cm), type II (multiple small cysts), and type III (microcystic). Adler et al. described a simplified classification based on gross appearance, and its use is recommended in fetal medicine:

(a) Macrocystic: One or more cysts measuring more than 5 mm

(b) Microcystic: Multiple cysts smaller than 5 mm

It usually affects one lung (95 %) but can be seen bilaterally, and both lungs can be affected. It is usually unilobar (85–95 %) and usually occurs in the lower lobes [38].

9.4.2.3 Imaging Findings

MRI findings are characteristic of fluid-filled structures, demonstrating bright T2 signal. A solid appearing lesion or a multicystic mass lesion with small or large cysts surrounded by abnormal hyperintense parenchyma is

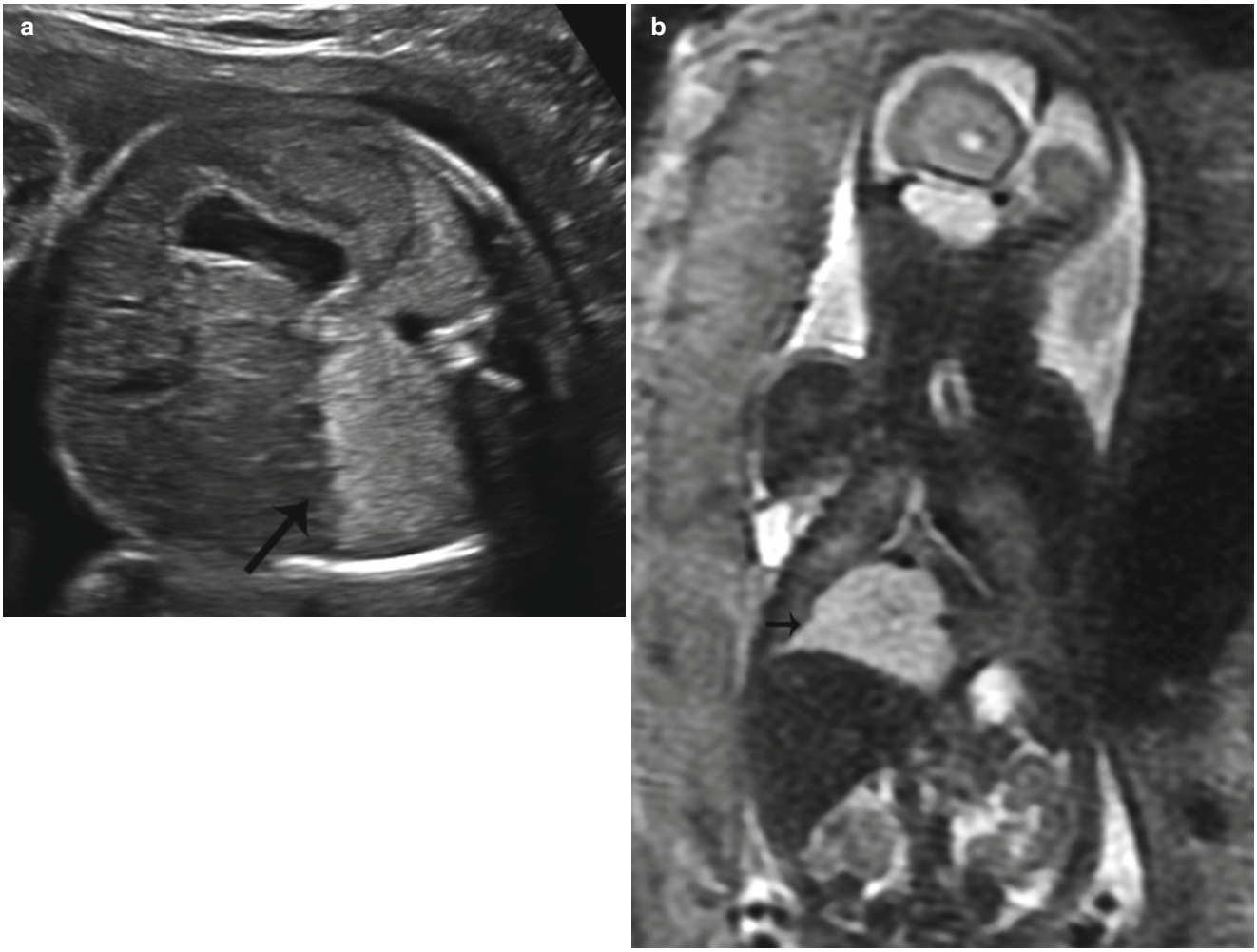

Fig. 9.5 Type III CPAM at 25 weeks gestation. (**a**) Axial US demonstrates an echogenic homogeneous mass in the right lower lobe (*arrow*). (**b**) Coronal SSFSE T2w image of the chest demonstrates a homogeneously high-signal mass in the right lower lobe (*arrow*). There was minimal mediastinal shift with a CVR of .4

appreciated in the thoracic cavity, depending on the type of CPAM (Fig. 9.5). The lesion exerts mass effect on the heart and other mediastinal structures causing heart rotation and shift to the contralateral side with different degrees of compression of venous structures and results in impaired venous return (Fig. 9.6). As a complication from mass effect and compression, pleural effusion, pericardial effusion, skin thickening, and/or ascites can develop (Fig. 9.7). Dilatation of the proximal esophagus can also be seen due to esophageal compression. As the fetus grows, the lesion becomes less conspicuous by ultrasound and can be better seen by MRI [3].

MRI allows evaluation of the residual normal lung and can sometimes be beneficial differentiating CPAM from other lung anomalies and identifying associated congenital anomalies [4, 39–41]. It can also help in differentiating between complete resolution and the presence of residual lesions, important for postnatal follow-up planning [7].

9.4.2.4 Prognosis and Fetal Management

Prognostic indicators include the size of the lesion, amount of mediastinal shift, and presence of polyhydramnios and/ or hydrops. Macrocystic lesions usually have a favorable prognosis, since most cases have a slow growth. When large, either macro- or microcystic, lesions can cause mediastinal shift and result in hemodynamical changes including polyhydramnios and nonimmune hydrops, which may require in utero intervention.

The CPAM volume ratio (CVR) [42], a measurement described by ultrasound, should be measured to assess prognosis and risk of hydrops. It is obtained by calculating the volume of the lung mass (height × anteroposterior diameter × transverse diameter × 0.52) and dividing it by the head circumference. A CVR <1.6 indicates a 14 % risk of developing hydrops for macrocystic lesions and 3 % for microcystic lesions. If CVR is >1.6, the risk increased to 75 % [42] (Fig. 9.8).

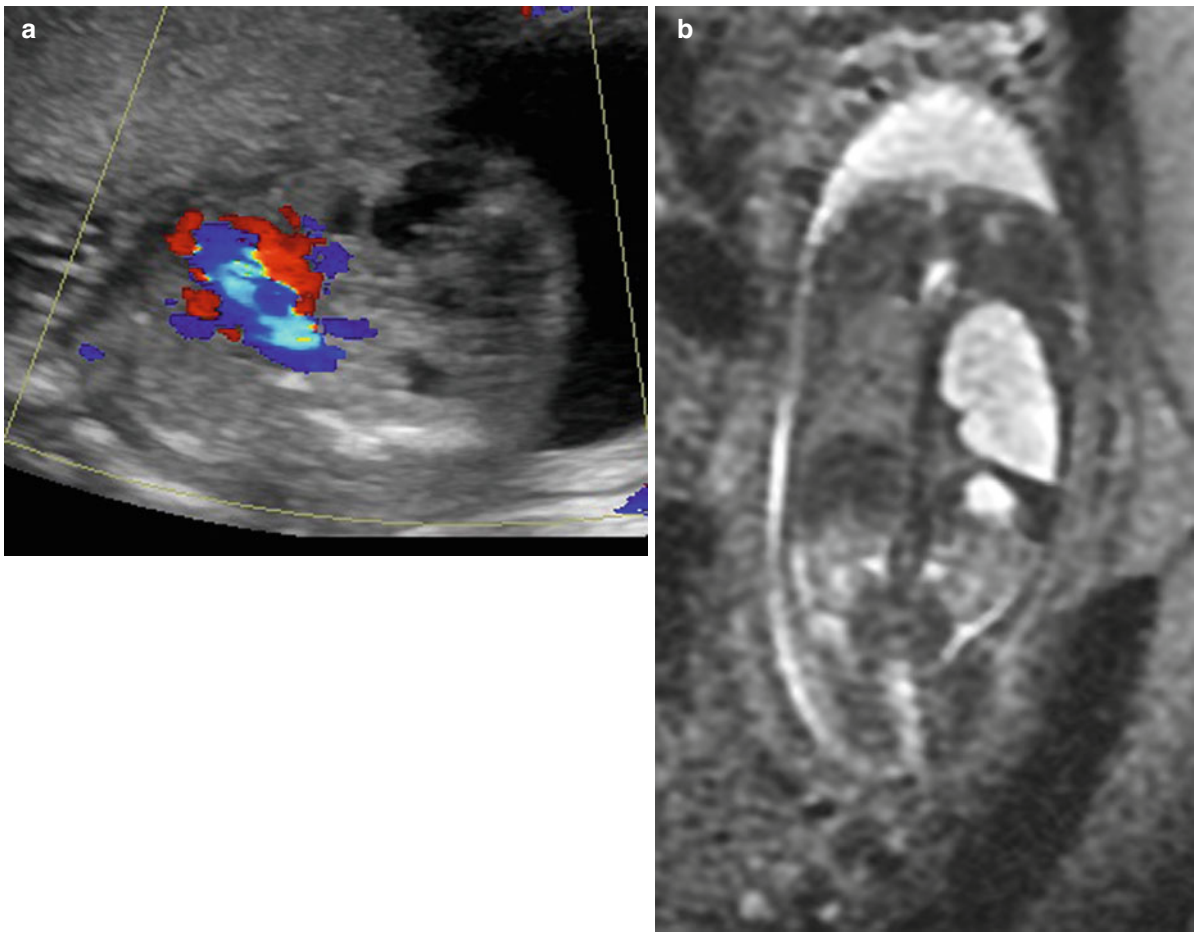

Fig. 9.6 Type 1 CPAM at 21 weeks gestation. (**a**) Axial US demonstrates macrocysts in the left lung deviating the heart (*color*) to the right. (**b**) Coronal SSFSE T2w image demonstrates that the cystic mass is in the left upper lobe

CPAM typically demonstrates an increase in size between 20 and 26 weeks of gestation and then plateaus [43]. It can later decrease in size [43] or seem to disappear due to similar signal intensity compared to normal lung parenchyma [44]. A residual mass can be seen in postnatal images in 40 % of cases when resolution by prenatal images was suspected.

Differential diagnosis includes BPS, CLO, bronchogenic cyst, CDH, laryngeal or tracheal occlusion, neurenteric/enteric cysts, and mediastinal teratomas.

Associated abnormalities and chromosomal abnormalities are seen in 8–20 % of patients, so a thorough examination should be performed [7, 45, 46].

9.4.3 Bronchopulmonary Sequestration (BPS)

9.4.3.1 Definition

BPS is a congenital anomaly of the lung characterized by a mass of nonfunctional lung tissue, usually affecting the lower lobes, without communication with the bronchial tree. Arterial supply to the mass is systemic and usually originates from the aorta, either lower thoracic or upper abdominal aorta. Other origins such as from the gastric artery and splenic artery can also occur [47].

9.4.3.2 Classification

BPS can be classified based on anatomical characteristics either intralobar (75 %) or extralobar (25 %) [48]. An intralobar lesion shares the visceral pleura of the rest of the normal lung, and venous blood drains into the pulmonary venous system; extralobar sequestration has its own visceral pleura, drains into the systemic veins, and is most commonly diagnosed in the prenatal or perinatal period [37, 48].

Based on location, the majority of BPS are supradiaphragmatic (85 %), and the remaining cases are either diaphragmatic or infradiaphragmatic (10 %) [37, 49]. Description of the location is important in order to provide a better differential diagnosis and follow-up evaluation; subdiaphragmatic lesions must be differentiated from neuroblastomas and adrenal hemorrhage [37, 48].

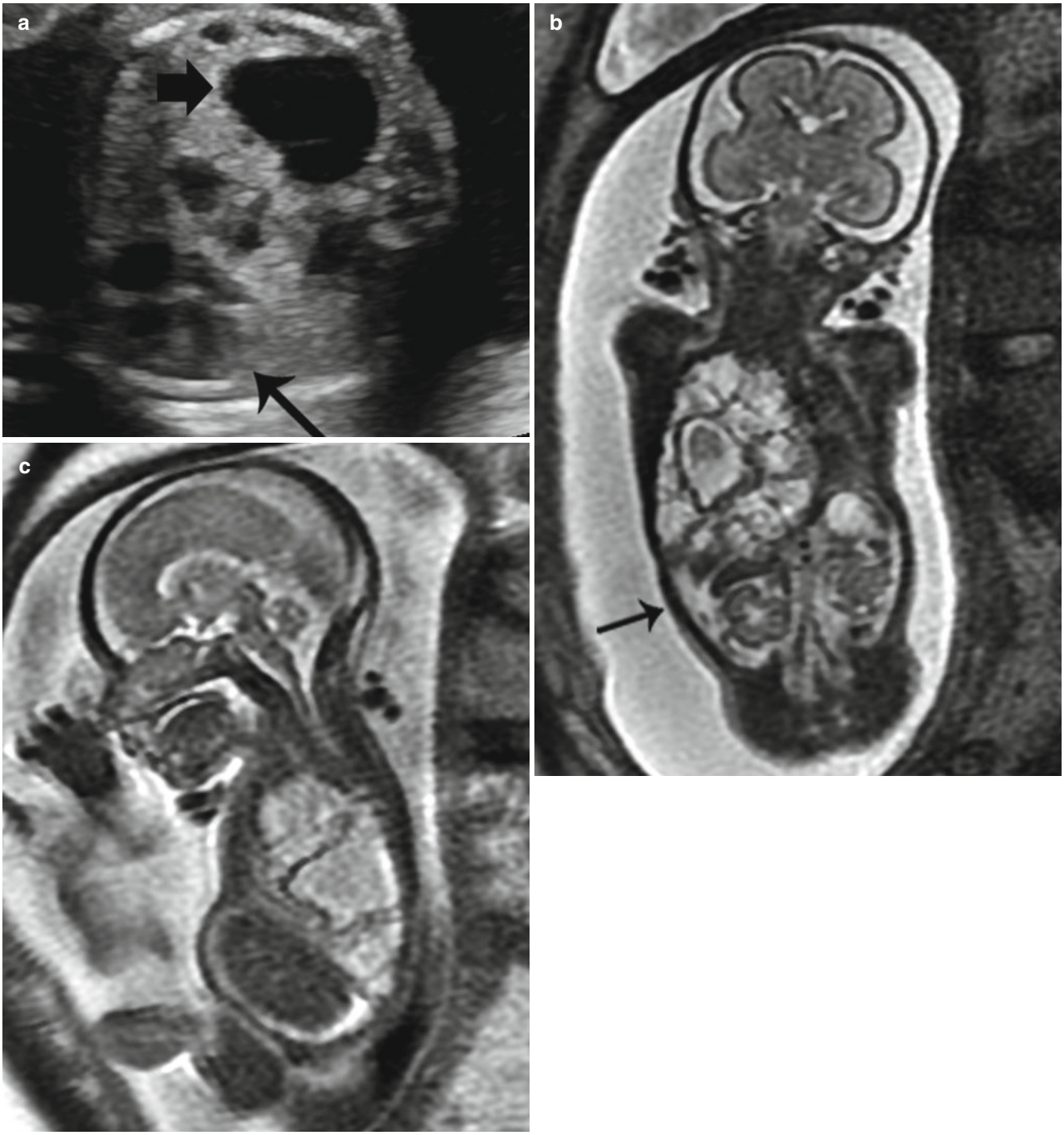

Fig. 9.7 Type 1 CPAM at 23 weeks gestation with ascites. (**a**) Axial US image demonstrates a right lung mass with scattered macrocysts (*thick arrow*) and surrounding echogenic tissue in the right lung deviating the heart (*thin arrow*) to the left. (**b**) Coronal and (**c**) Sagittal SSFSE MR images of the chest demonstrate macrocysts deviating the diaphragm inferiorly. Ascites is present (*arrow*). CVR measured was 2.3. The fetus survived following intrauterine drainage of several cysts

When a BPS coexists with a CPAM, it is called a hybrid lesion, and they can have both systemic and pulmonary arterial feeders (Fig. 9.9). 25–50 % of extralobar sequestrations are hybrid lesions [36].

9.4.3.3 Imaging Findings

MRI demonstrates a well-defined, wedged-shaped lung mass that is hyperintense on T2-weighted sequences. A low-signal linear structure representing the lung mass feeder can

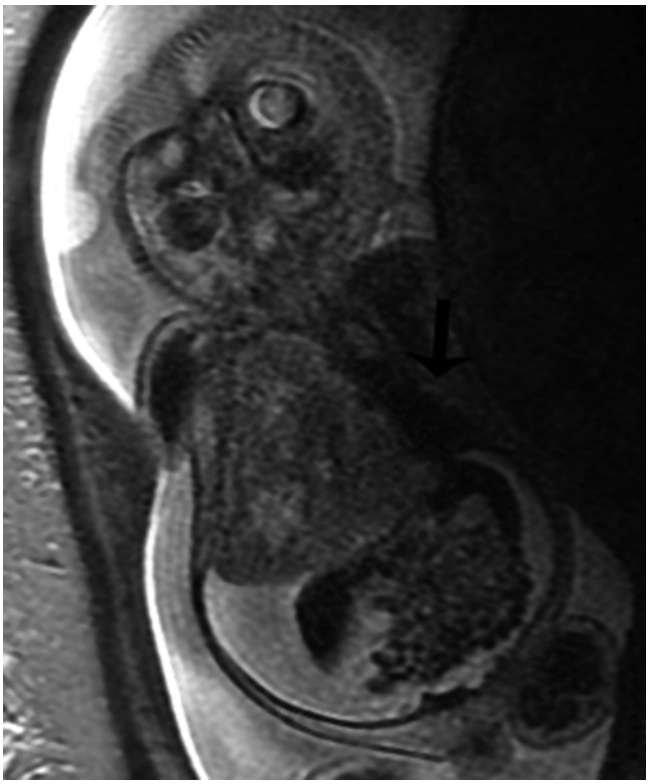

Fig. 9.8 Type III CPAM with hydrops at 28 weeks gestation. Coronal SSFSE MR image demonstrates a large heterogeneous mass in the right thorax deviating the heart to the left (*arrow*). CVR was 5. There is diffuse skin edema and ascites. The fetus died despite steroid therapy

sometimes be seen by MRI but is usually better seen by ultrasound, by power and color Doppler (Fig. 9.10). MRI is beneficial in the delineation and better localization of the mass. MRI also allows for better evaluation of the contralateral lung and in the assessment of associated congenital anomalies.

Follow-up MRI may demonstrate a smaller lesion with hypointense T2 signal compared to the lung if the lesion either decompressed into the lung, outgrew the systemic circulation, or had a vascular/lymphatic obstruction due to torsion [50].

9.4.3.4 Prognosis and Fetal Management

Prognosis depends on the size of the lesion and presence of hydrops. When the mass is large, it can cause mass effect on the mediastinal structures. If significant compression is exerted on the heart and venous structures, hydrops can occur; if the esophagus is compressed, polyhydramnios can be seen [41, 50, 51]. Most have a good prognosis since the majority decreases in size in utero (75 %), and hydrops is rarely seen [4, 41, 48, 50]. If hydrops develops as a complication, the survival decreases to 20–30 % [50].

Serial follow-up examinations should be performed. The majority (75 %) of prenatally diagnosed BPS decreases in size and becomes harder to see by ultrasound, but an increase in size can also be seen. Follow-up examinations are performed with ultrasound for reevaluation of the lesion, change in size, variation in mediastinal compression, and presence of hydrops. Closer follow-up is recommended for larger lesions given with higher risk for hydrops. Late MRI can be performed to better delineate the feeding vessels, with a better correlation with postnatal imaging [52]. In some institutions, postnatal imaging is not performed if prenatal MRI properly depicts the feeding vessel for surgical planning.

Thorough examination of the entire fetus should be performed looking for associated congenital anomalies, especially in the presence of a suspected extralobar type. Fetal karyotype should be recommended if fetal intervention could be considered in the future management.

Fetal intervention is indicated in the presence of hydrops earlier in pregnancy and significantly increases survival [51, 53]. If hydrops develops after weeks 32–34, early delivery and postnatal management is an option [41].

Different fetal interventional techniques have been performed, including thoracentesis as a temporizing option, thoracoamniotic shunt, percutaneous laser ablation, and in utero open resection; for delivery, ex utero intrapartum therapy can be offered if needed [41, 53–62].

9.4.4 Congenial Lobar Overinflation (CLO)

9.4.4.1 Definition

CLO is a rare entity characterized by overinflation of the lung. It is usually unilateral and usually affects one lobe; involvement of more pulmonary lobes [63] and bilateral lesions has been described.

In neonates who present with respiratory distress, the left upper lobe is most commonly affected followed by right middle and right upper lobes; in prenatal cases, a predisposition for lower lobe involvement and a high association with bronchial atresia have been seen [37]. It is also known as congenital lobar emphysema, though no damage to the alveolar wall is appreciated [37].

9.4.4.2 Classification

CLO can be idiopathic in about 50 % of cases [63]. The remaining 50 % can be extrinsic or intrinsic in origin. Intrinsic factors include cartilaginous deficiency, bronchial stenosis/atresia, or mucus plugs. Extrinsic causes include extrinsic compression from an extrabronchial mass or vascular structure such as dilated pulmonary arteries in tetralogy of Fallot with the absent pulmonary valve (Fig. 9.11).

9.4.4.3 Imaging Findings

CLO is characterized as an area of increased T2 signal with a lobar distribution; it is usually more homogeneous than

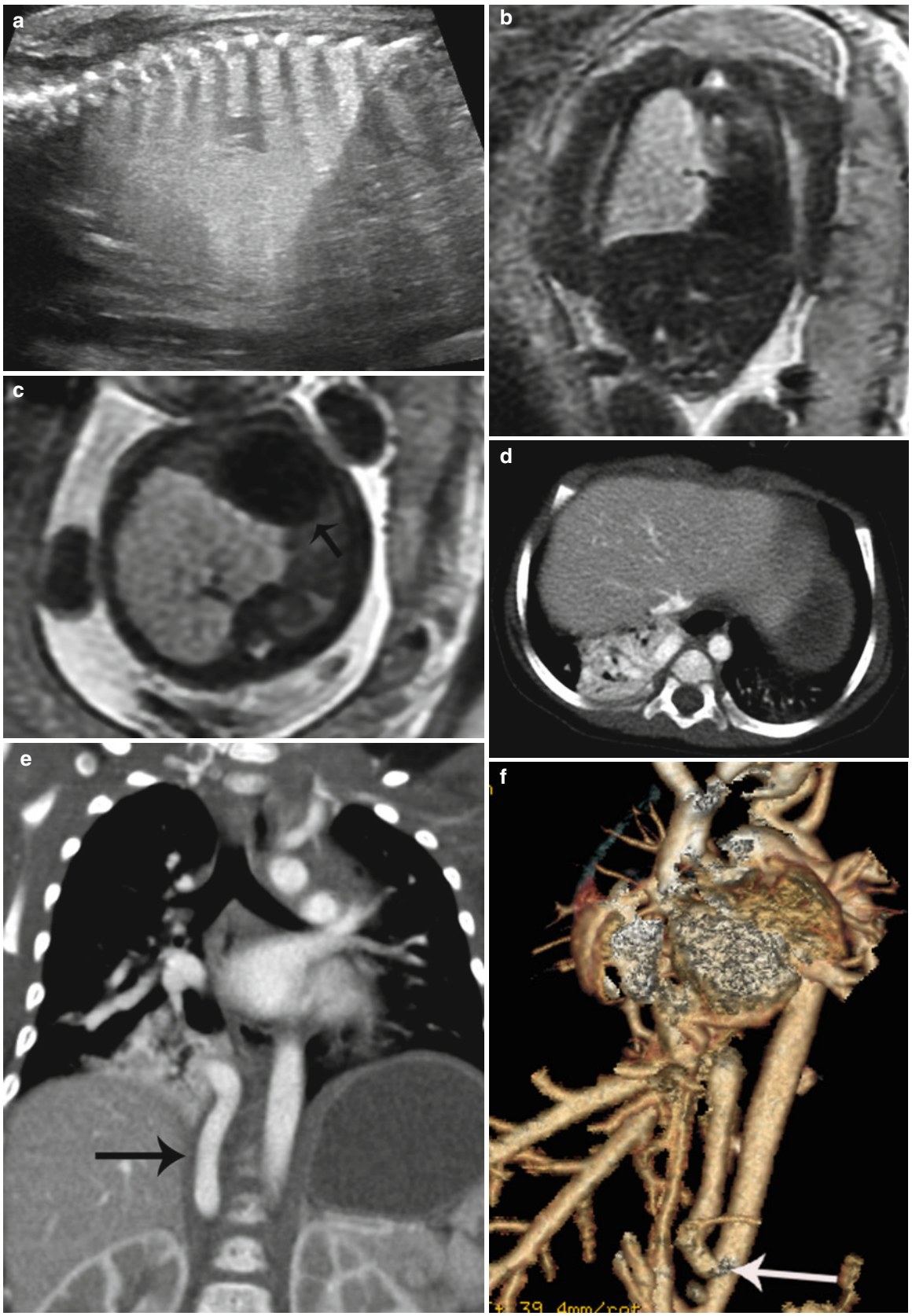

Fig. 9.9 Hybrid CPAM BPS at 23 weeks gestation. (**a**) Sagittal US image demonstrates a large echogenic mass inverting the diaphragm. A few macrocysts are noted centrally. (**b**) Coronal and (**c**) axial SSFSE MR images demonstrate a high-signal mass deviating the heart to the right (*arrow*). CVR was 1.7. No definite systemic feeding vessel was identified. Patient was asymptomatic at delivery. (**d**) Axial CT at 6 months of age demonstrates a vascular mass in the right lower lobe. (**e**) Coronal reconstruction reveals a large infradiaphragmatic systemic feeding vessel (*arrow*) coursing into the mass. (**f**) 3D reconstruction demonstrates a large feeding vessel (*arrow*) branching off the celiac axis

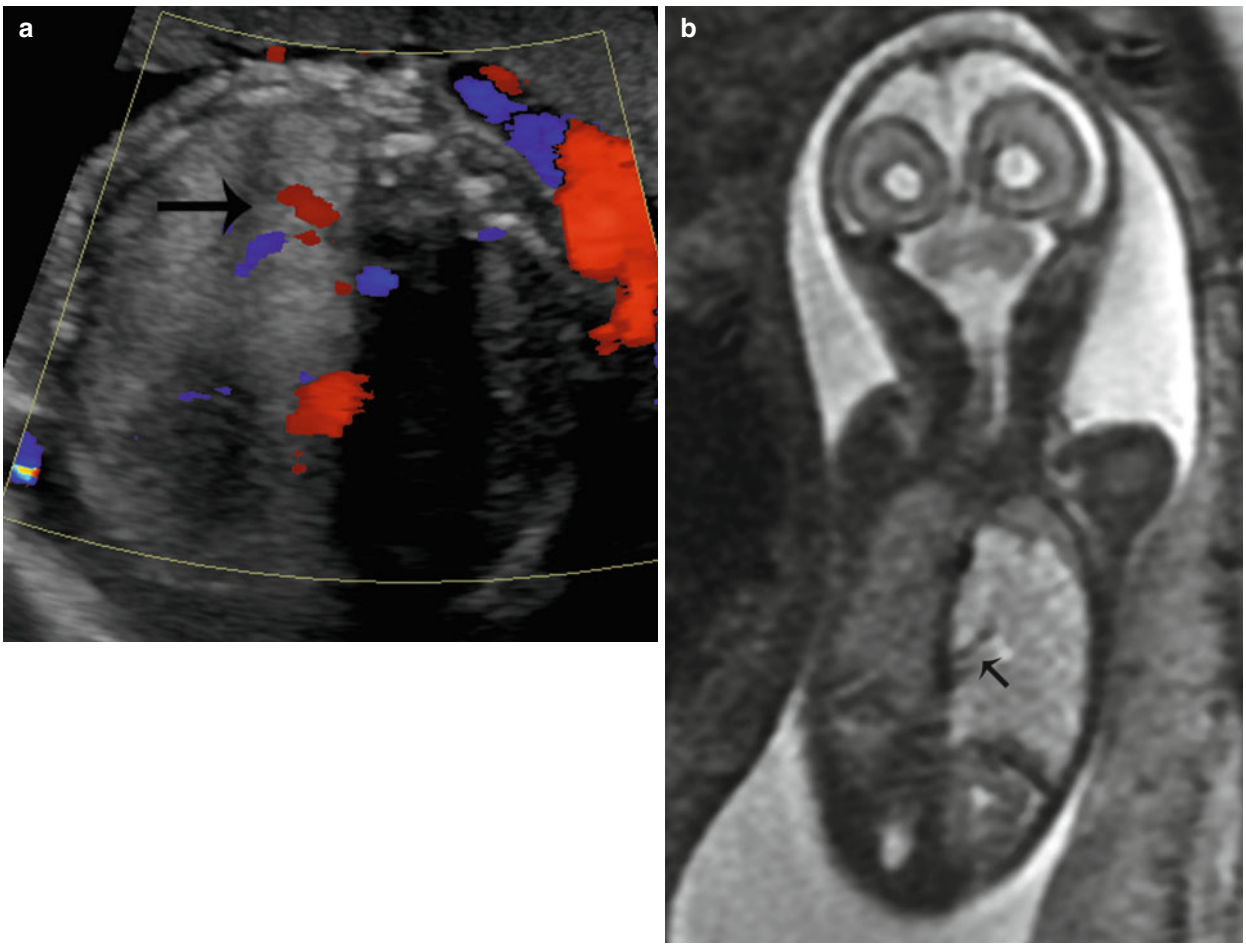

Fig. 9.10 Bronchopulmonary sequestration at 27 weeks gestation. (**a**) Axial US demonstrates an echogenic solid mass in the left lower lobe with a systemic feeding vessel (*arrow*) branching from the descending aorta. (**b**) Coronal SSFSE T2w confirms the left lower lobe mass with systemic feeding vessels (*arrow*) coursing into the mass

CPAM and less hyperintense when compared to BPS [48]. Lung structure appears intact with stretched hilar vessels [64].

When the overinflated lung is large, mediastinal shift and adjacent normal lung compression can occur [65], and herniation of the overinflated lung can be seen to the contralateral side [66].

9.4.4.4 Prognosis and Fetal Management

Echocardiogram should be performed to exclude congenital heart disease. 14 % of patients have an associated cardiac anomaly, most likely a large left to right shunt with pulmonary hypertension [65].

Prenatal outcome varies from spontaneous resolution to progression with increase in size and increased intrathoracic pressure resulting in impaired fetal circulation and swallowing with hydrops and polyhydramnios. Occasionally, resolution is suspected prenatally, but a persistent, nonvisualized mass could result in neonatal respiratory insufficiency due to presence of overinflation and valve mechanism [63].

The main indicator of prenatal outcome is the presence of hydrops, and follow-up examinations should be performed to assess changes and presence of hydrops.

9.4.5 Congenital Hydrothorax

9.4.5.1 Definition

The presence of pleural fluid is considered abnormal in the fetus. It can be seen in isolation or in association with a lesion, such as CPAM, BPS, lymphangiectasia, cardiac anomalies, infections including TORCH, and chromosomal abnormalities like Turner syndrome and trisomy 21.

9.4.5.2 Classification

Hydrothorax can be primary or secondary. Primary hydrothorax is rare and affects males more frequently. It results from an anomaly in the development of the lymphatic system resulting in chylous leak into the pleural space and can be unilateral or bilateral [67, 68]. Primary effusions are

Fig. 9.11 Congenital lobar overinflation at 35 weeks gestation. Coronal SSFSE T2w image demonstrates a hyperexpanded high-signal right lower lobe deviating the heart to the left with flattening of the right hemidiaphragm. The fetus had tetralogy of Fallot with absent pulmonary valves causing trapping of fluid

characterized by having high pressures, resolving rapidly after thoracentesis and developing hydrops restricted to the upper fetal body [68]. Secondary hydrothorax is seen in hydrops-related pathologies or pulmonary masses that can cause mass effect and compression.

9.4.5.3 Imaging Findings

When a hydrothorax is present, MRI demonstrates an area of bright T2 signal surrounding the lung parenchyma. It can be small or large and unilateral or bilateral and can remain stable, resolve, or progress to hydrops. Depending on the size, mediastinal shift and lung compression can occur (Fig. 9.12). MRI may help identify associated abnormalities not seen by ultrasound, like an inconspicuous CPAM or BPS.

Depending in the content of the pleural fluid (lipid, protein, or blood products), different signal intensities might be seen with MRI in both T1- and T2-weighted images that may help establish the etiological diagnosis [7].

Fig. 9.12 Congenital hydrothorax at 30 weeks gestation. Axial SSFSE image of the chest demonstrates a large left pleural effusion (*arrow*) deviating the heart to the right and compressing the ipsilateral lung. There is compression of the contralateral right lung as well

Ultrasound is the modality of choice for follow-up examinations. An effusion ratio can be obtained by ultrasound (area of effusion divided by area of thorax) and followed with serial examinations; if it elevates, it suggests evolution to hydrops [69], but no cutoff ratio has demonstrated usefulness as a prognostic tool [68].

9.4.5.4 Prognosis and Fetal Management

Thorough fetal assessment for associated anomalies, including echocardiograph, maternal serology for infections, and fetal karyotyping, is recommended [68, 70].

Prognosis depends on the presence of associated abnormalities, whether it is unilateral or bilateral, and on the size of hydrothorax and presence of mediastinal shift. Small primary hydrothorax can have spontaneous resolution in 22 % of cases [68]. Unilateral effusions, spontaneously resolved effusions, and those without mediastinal shift or hydrops have a 73–100 % survival [68, 71]. Progression from unilateral to bilateral is a sign of impending hydrops [67]. When large, bilateral, and with mediastinal shift, mortality decreases to 52 % [71], and when progression to hydrops is seen, mortality increases to 62 % [71].

Secondary hydrothorax has a worse outcome. Mortality in these cases can be up to 98 % depending on size, progression to hydrops, and underlying cause [71].

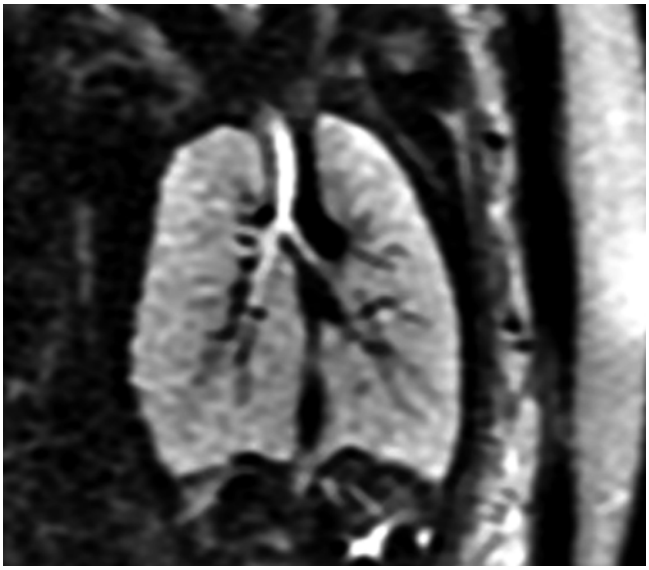

Fig. 9.13 Congenital high airway obstruction (CHAOS). Coronal SSFSE T2w image demonstrates large high-signal lungs with flattening of the diaphragms. Fluid fills the dilated trachea and bronchi in this fetus with tracheal obstruction

Fetal intervention includes serial thoracentesis and thoracoamniotic shunt placement. Uterochemical pleurodesis has also been tried [67].

9.4.6 Congenital High Airway Obstruction Syndrome (CHAOS)

9.4.6.1 Definition

CHAOS is a rare congenital anomaly that affects the trachea or larynx and results in atresia, stenosis, or web formation of the airway with distal overexpansion of the lungs. Significant increase in the size of the lungs is noted, which results in compression of the heart and inferior vena cava with impaired venous return and hydrops.

9.4.6.2 Imaging Findings

MRI demonstrates increased lung volumes with diffuse increased T2 signal due to higher fluid content (Fig. 9.13). The large lungs cause flattening or inversion of the diaphragm, anterior displacement of a small heart, and hydrops. Dilatation of the airway to the level of the obstruction is present and is important for surgical planning. Placentomegaly is also appreciated [72].

MRI is increasingly used in the evaluation of these patients, it is considered to be superior compared to ultrasound in confirming the level of the obstruction, and it helps exclude causes of extrinsic compression as well as assists in exclusion of differential diagnosis [73] (Fig. 9.14).

Fig. 9.14 Bronchogenic cyst causing airway obstruction. Coronal SSFSE T2w image demonstrates large high-signal lungs with flattening of the diaphragms. A mediastinal multilobulated cystic structure is causing obstruction of the bronchi at the carina. The bronchi are dilated and fluid filled but the trachea is not

9.4.6.3 Prognosis and Fetal Management

Without prenatal diagnosis and early treatment, CHAOS has a high mortality (80–100 %) [72].

EXIT procedure may be offered to secure an adequate airway below the level of obstruction during delivery. High perinatal mortality and abnormal respiratory function in survivors are seen, even after successful EXIT procedure [74]. Different fetal interventional procedures have been done in an attempt to increase survival, including opening the airway by open surgery or fetoscopy [74]. Best prognosis is seen in patients whose airway can be visualized, and an isolated subglottic membrane appears to be the origin since fetoscopy with deobstruction can be a curative procedure [74].

A less severe subtype without hydrops has been described with improvement/resolution of the imaging findings [73, 75]. These cases have a pharyngotracheal or laryngotracheal fistula that allows partial decompression of the airway not to resolution of the primary pathology [73].

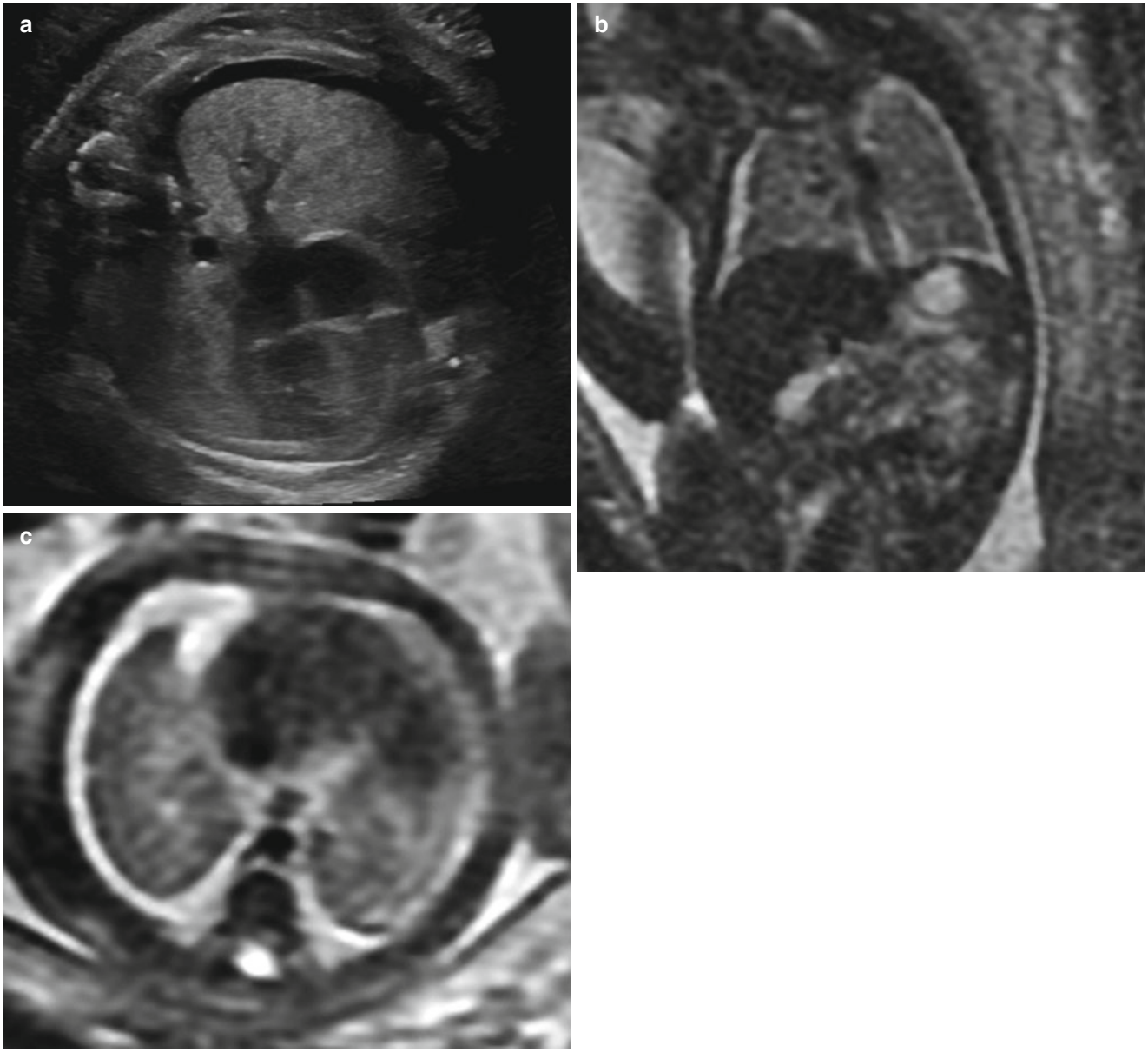

Fig. 9.15 Pulmonary lymphangiectasia at 28 weeks gestation. (**a**) Axial US of the chest demonstrates small bilateral pleural effusions with slightly heterogeneous parenchyma. Coronal (**b**) and axial (**c**) SSFSE T2w images demonstrate small bilateral pleural effusions and heterogeneous signal throughout both lungs termed "nutmeg lung." Branching hyperintense structures emanate from the hila of both lungs

9.4.7 Pulmonary Lymphangiectasia

9.4.7.1 Definition

Pulmonary lymphangiectasia is a congenital disease resulting in the obstruction and dilation of the pulmonary lymphatic system of unknown etiology. The lungs become enlarged and noncompliant, with effusions that may lead to respiratory distress at delivery.

9.4.7.2 Classification

Primary and secondary forms of pulmonary lymphangiectasia have been described. The secondary form occurs as a result of congenital heart disease causing poor venolymphatic return [76, 77].

9.4.7.3 Imaging Findings

Ultrasound images show pleural effusions and a heterogeneous lung parenchyma (Fig. 9.15).

Fetal MRI also demonstrates the pleural effusions and lung heterogeneity, but a typical heterogeneous pattern termed the "nutmeg lung" is usually seen, thus providing a more specific diagnosis. MRI also helps exclude other lung masses. Branching tubular T2-hyperintense structures can be seen radiating from the hila [77].

9.4.7.4 Prognosis and Fetal Management

Cardiac echo is important to exclude cardiac anomalies.

Postnatal management includes different attempts at reducing pulmonary lymph burden such as restriction of dietary fats, pleural effusion drainage, pleurodesis, and more invasive procedures such as thoracic duct ligation. Recent experimental treatment using ethiodized oil to embolize the patulous pulmonary lymphatics has shown some success [78].

9.4.8 Pulmonary Hypoplasia/Aplasia/Agenesis

9.4.8.1 Definition

Arrest in lung development results in pulmonary hypoplasia, pulmonary aplasia, or pulmonary agenesis depending on the time of the arrest and resultant amount of absent parenchyma.

Pulmonary hypoplasia is the presence of an underdeveloped lung, small in size and with decreased weight, characterized by a decreased number of alveoli and bronchi. Pulmonary aplasia is the presence of rudimentary bronchi with no associated lung parenchyma. Pulmonary agenesis is the complete absence of bronchi, pulmonary vessels, and lung parenchyma [79].

Left-sided pulmonary agenesis is the most common, seen in 70 % of cases [79].

9.4.8.2 Classification

Pulmonary hypoplasia can be primary or secondary. Majority of cases of lung hypoplasia are seen secondary to oligohydramnios with or without renal origin, lung masses, congenital diaphragmatic hernia, skeletal dysplasias, and other entities that restrict normal lung expansion and development (Fig. 9.16). Primary pulmonary hypoplasia is less common and can be associated with other abnormalities, such as seen in VACTERL association and venolobar (scimitar) syndrome (Fig. 9.17).

Pulmonary agenesis is usually unilateral and can affect the right or left lung. Occasionally, it is bilateral and incompatible with life.

9.4.8.3 Imaging Findings

In pulmonary hypoplasia, MRI demonstrates hypointense T2 signal of the hypoplastic lung in comparison with normal lung appearance. The progressive hyperintensity typically seen during pregnancy is not appreciated [80]. When oligohydramnios is present and ultrasound images are limited, the benefit of prenatal MRI is significant in helping to establish the etiology of oligohydramnios and the degree of lung involvement.

In unilateral pulmonary hypoplasia or agenesis, the hemithorax is small. With agenesis, there is no visualization of the ipsilateral lung, bronchus, and pulmonary artery. Associated significant ipsilateral deviation of the mediastinum is noted, and a contralateral homogeneous normal appearing lung is seen (Fig. 9.18).

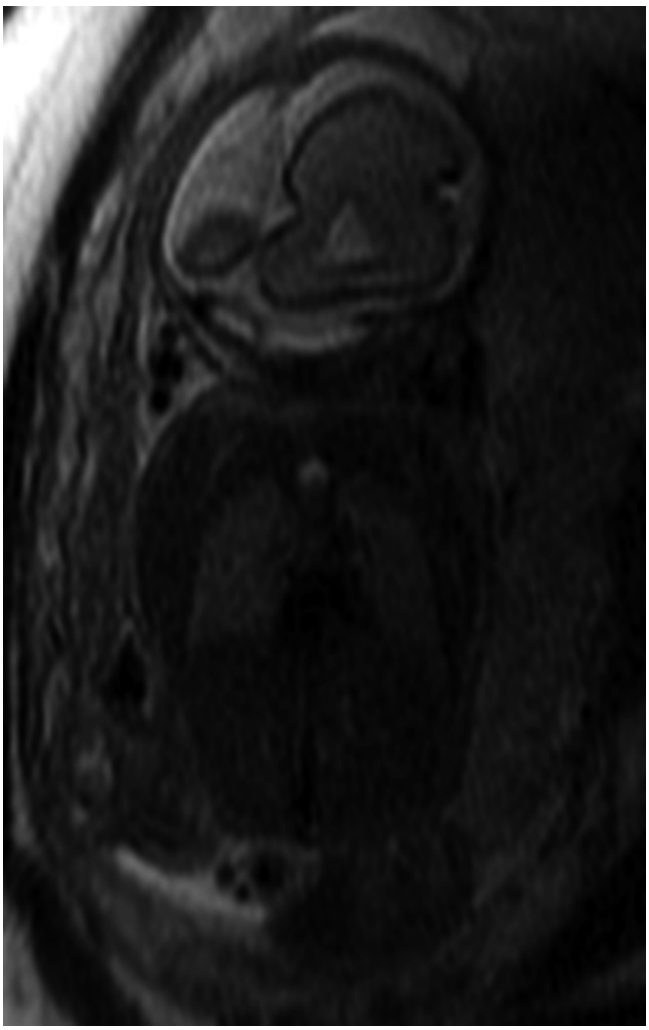

Fig. 9.16 Pulmonary hypoplasia at 27 weeks gestation. Coronal SSFSE T2w image demonstrates severe oligohydramnios. The lungs are small and low in signal for gestational age. The fetus had bilateral renal agenesis

In bilateral pulmonary agenesis, the MRI will demonstrate a significantly decreased thoracic volume with bilateral elevation of the diaphragms and upward migration and rotation of the heart [81–83]. Ultrasound evaluation usually makes the diagnosis and can demonstrate absence of major pulmonary vessels; MRI is beneficial confirming the diagnosis and excluding other pathologies [79].

9.4.8.4 Prognosis and Fetal Management

Prognosis of lung hypoplasia depends on etiology and the age at onset. Pulmonary vascularity develops at the same time as the alveoli, and thus abnormal pulmonary vessels can be associated with hypoplastic alveoli.

Unilateral pulmonary agenesis may have a good survival; however, more than 50 % of patients with lung agenesis have an associated congenital anomaly that could decrease survival [79, 81]. Lung agenesis can occur on the right or left

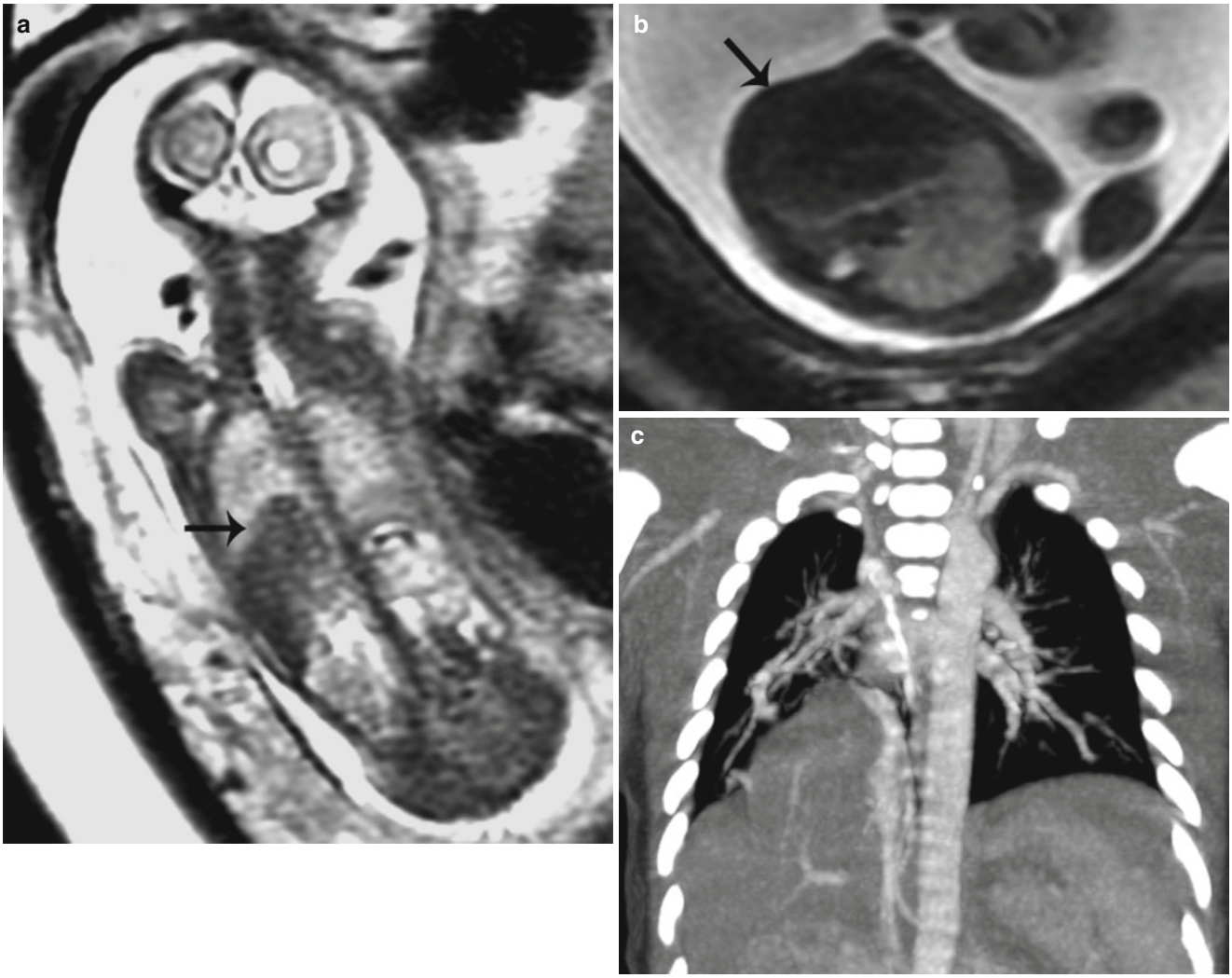

Fig. 9.17 Venolobar (scimitar) syndrome. (**a**) Coronal SSFSE T2w image at 22 weeks gestation demonstrates an elevated right hemidiaphragm (*arrow*). (**b**) Axial SSFSE image, however, demonstrates the mediastinum to be shifted to the right (*arrow*) implying the right lung is hypoplastic. (**c**) Coronal CTA at 2 days of age demonstrates a hypoplastic right lung with an anomalous right pulmonary vein coursing to the abdomen

side, but higher mortality has been seen in patients with right-sided agenesis, likely secondary to more severe mediastinal shift, vascular/bronchial distortion, and increased association with congenital anomalies [79].

9.5 Other Thoracic Lesions

9.5.1 Bronchogenic Cyst

A bronchogenic cyst originates from abnormal budding of the tracheobronchial tree. Bronchogenic cysts are usually too small to be well delineated by prenatal imaging [4].

They can present as mediastinal or parenchymal lesions. Mediastinal lesions consist of a unilocular cystic lesion, located near midline in the subcarinal region (75 % of cases). Parenchymal lesions are usually unilocular simple cysts within normal lung parenchyma, along the tracheobronchial tree (Fig. 9.19). Though by imaging they are usually simple cysts with hyperintense T2 signal, septations can be seen with ultrasound and occasionally can cause bronchial compression and result in distal lung overinflation with hyperintense T2 signal (Fig. 9.14).

Most cysts are well tolerated in utero [35].

9.5.2 Cystic Pleuropulmonary Blastoma (CPPB)

Pleuropulmonary blastoma (PPB) is a rare primary neoplasm originating from the pleuropulmonary mesenchyme (previously called pulmonary blastoma and malignant mesenchymoma among other multiple names) [83]. Three types of pleuropulmonary blastoma have been described: type I is

Fig. 9.18 Left pulmonary agenesis at 33 weeks gestation. Coronal SSFP T2w image demonstrates complete shift of mediastinal structures into the left hemithorax. The right lung is homogeneous and partially shifted to the left as well. Note the multicystic dysplastic right kidney in this fetus with VACTERL association

exclusively cystic, type II is a mixed cystic and solid lesion, and type III is a predominantly solid mass.

CPPB presents as a complex macrocystic lesion in the chest, indistinguishable from a CPAM. Features that should raise concern and help differentiate from a prenatal CPAM include: (1) positive family history, (2) multifocal lesions, and (3) association with pleural effusion [37]. There are no specific imaging findings or other preoperative tests to distinguish type I CPPB from type I CPAM [83]. Progressive enlargement in the third trimester or postnatally is worrisome for a CPPB unlike CPAM which regresses over time.

Outcome is dependent on early diagnosis and complete resection [83].

9.5.3 Neurenteric/Duplication Cyst

Rare cystic thoracic lesions of the fetus include neurenteric or duplication cysts. They usually present as unilocular cystic lesions near the midline. Thorough evaluation for associated vertebral abnormalities should be performed, though may be difficult to diagnose prenatally [4].

9.5.4 Lymphangiomas

Lymphatic malformations are secondary to failure in the development of local lymphatics. They appear as multilocular cystic lesions and rarely have solid components [72].

Lymphatic malformations usually are located in the neck (75 %), most likely arising from the posterior aspect, and in the axilla (20 %) involving the lateral chest wall; approximately 10 % extends into the mediastinum [72, 84]. One percent can be confined to the mediastinum and usually present in the anterior and superior mediastinal regions [84]. Chest lymphangiomas are not associated with chromosomal abnormalities and usually present later in pregnancy [84, 85].

MRI studies demonstrate a heterogeneous hyperintense T2 signal lesion (Fig. 9.20). Ultrasound may better demonstrate the septations. Lymphangiomas are variable in size and have a slow growth; however, a rapid increase in size can occur – secondary to hemorrhage prenatally or infection postnatally – which could lead to lung compression, hypoplasia, mediastinal shift, and hydrops [84].

9.5.5 Mediastinal Teratoma

Mediastinal teratomas are rarely seen in utero [4, 86]. They are usually seen as an anterior mediastinal complex mass of mixed heterogeneity with or without internal calcifications (better seen by ultrasound) [87]. The mass can cause polyhydramnios secondary to esophageal compression, hydrops due to impaired venous return and fetal demise [86]. After delivery, respiratory distress can occur.

Fetal intervention with aspiration of the tumor cyst has been described with a resultant decrease in intrathoracic pressure, which may stop the progression to hydrops and prevent lung hypoplasia. EXIT procedure is recommended to establish a proper airway at delivery [86].

9.5.6 Mesenchymal Hamartoma of the Chest Wall

Mesenchymal hamartomas are infrequent benign tumors of infancy and extremely rare in the prenatal period. They usually originate from the posterior wall and may affect multiple adjacent ribs. They may be multifocal and bilateral.

Ultrasound demonstrates a heterogeneous mass with a peripheral echogenic capsule with posterior acoustic shadowing suggestive of calcified rim [87].

Fig. 9.19 Bronchogenic cyst. Coronal (**a**) and sagittal (**b**) SSFSE T2w images of the chest demonstrate a high-signal cyst in the middle mediastinum. The lung parenchyma appeared normal. (**c**) Postnatal CT confirms the presence of a bronchogenic cyst

By MR imaging, they are heterogeneous thoracic masses, located in the costal region. They are expansive and demonstrate molding and erosion of osseous structures and have an associated extrapleural mass of soft tissue. They can be associated with pleural effusion due to bleeding [88]. When large, lung compression with postnatal respiratory compromises and/or scoliosis can be present [87].

9.5.7 Congenital Pulmonary Fibrosarcoma

It is also known as congenital peribronchial myofibroblastic tumor. It is a rare lung tumor, usually with benign histology that affects the fetus or newborn [37, 89].

It presents as a very large, solid lung mass with low-signal intensity demonstrated on both T1- and T2-weighted sequences due to high fibrous content. No

Fig. 9.20 Lymphangioma at 21 weeks gestation with subcutaneous lymphangioma diffusely. Septated lymphangiomas can be noted within the mediastinum surrounding the great vessels as well (*arrow*)

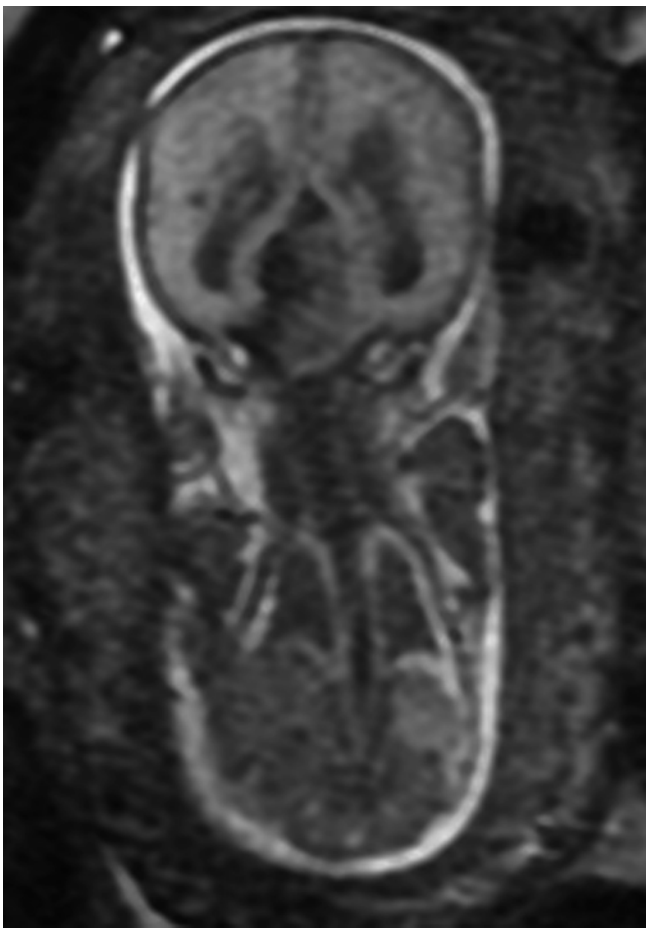

Fig. 9.21 Fetal demise at 29 weeks gestation referred for growth retardation, oligohydramnios, and cranial anomaly. Coronal SSFSE image demonstrates oligohydramnios with small bilateral pleural effusions. The lung parenchyma is low in signal for gestational age. There is loss of gray white matter differentiation. No fluid-filled stomach or bladder was noted

feeding vessel is identified to suggest BPS, and no hyperintensity of T2 to suggest bronchopulmonary malformation. This tumor usually presents with hydrops and can result in fetal demise or respiratory distress at birth [89]. If no metastatic disease is present, surgical resection can be curative [37].

9.6 Fetal Demise

At times, MRI may be performed on an unexpected fetal demise. Within the chest, a decrease in lung volume is appreciated with associated bilateral pleural effusion (Fig. 9.21). The heart chambers are small in size and there is loss of flow void within. Diffuse skin edema is present. Other extrathoracic findings include loss of gray white matter differentiation in the brain, small and elliptical orbital globes with dark rim, and nonvisualization of the stomach and bladder. There is an overall diffuse homogeneity of the fetus because of edema and less tissue differentiation [90].

Conclusion

A wide variety of congenital anomalies affect the thoracic region of the fetus. They can be small and asymptomatic or large and cause mass effect, with outcomes that vary significantly depending on associated anomalies and presence of complications such as lung hypoplasia and hydrops. These complications are of significant importance in the prognosis of the fetus.

Ultrasound remains the first modality of choice in the evaluation of the fetus and diagnosis of congenital abnormalities. MRI has become a useful adjuvant in the evaluation of thoracic abnormalities. Advantages as discussed in this chapter include:

- Multiplanar capability and large field of view with excellent tissue contrast resolution – providing a better image of the pathology and increasing confidence in diagnosis facilitating counseling and treatment planning.

- Improved assessment of lung volumes and herniated liver volumes in hypoplastic lungs and congenital diaphragmatic hernias.
- Third trimester MR can help plan for postnatal care obviating the need for additional postnatal imaging which could require radiation and/or sedation.

Lastly, it is hoped that in the near future, innovative MR sequences such as diffusion-weighted imaging and spectroscopy may provide additional information regarding lung function and maturity.

References

1. Kul S, Ata Korkmaz HA, Cansu A et al (2012) Contribution of MRI to ultrasound in the diagnosis of fetal anomalies. J Magn Reson Imaging 35:882–890
2. Breysem L, Bosmans H, Dymarkowski S et al (2003) The value of fast MR imaging as an adjunct to ultrasound in prenatal diagnosis. Eur Radiol 13:1538
3. Levine D, Barnewolt CE, Mehta TS et al (2003) Fetal thoracic abnormalities: MR imaging. Radiology 228:379–388
4. Hubbard AM, Adzick NS, Crombleholme TM et al (1999) Congenital chest lesions: diagnosis and characterization with prenatal MR imaging. Radiology 212:43
5. We JS, Young L, Park IY et al (2012) Usefulness of additional fetal magnetic resonance imaging in the prenatal diagnosis of congenital abnormalities. Arch Gynecol Obstet 286:1443–1452
6. Moore RJ, Stradchan B, Tyler DJ et al (2001) In vivo diffusion measurements as an indication of fetal lung maturation using echo planar imaging at 0.5T. Magn Reson Med 45:247–253
7. Cannie M, Jani J, De Keyzer F et al (2008) Magnetic resonance imaging of the fetal lung: a pictorial essay. Eur Radiol 18:1364–1374
8. Laudy JA, Wladimiroff JW (2000) The fetal lung. 1: developmental aspects. Ultrasound Obstet Gynecol 16(3):284–290
9. Burri PH (2006) Structural aspects of postnatal lung development – alveolar formation and growth. Biol Neonate 89(4):313–322
10. Leeuwen L, Fitzgerald DA (2014) Congenital diaphragmatic hernia. J Paediatr Child Health 50:667–673
11. Graham G, Devine C (2005) Antenatal diagnosis of congenital diaphragmatic hernia. Semin Perinatol 20:69–76
12. Hidaka N, Ishii K, Mabuchi A et al (2015) Associated anomalies in congenital diaphragmatic hernia: perinatal characteristics and impact on postnatal survival. J Perinat Med 43(2):245–252
13. Claus F, Sandalite I, Dekoninck P et al (2011) Prenatal anatomical imaging in fetuses with congenital diaphragmatic hernia. Fetal Diagn Ther 29(1):88–100
14. Wynn J, Yu L, Chung WK (2014) Genetic causes of congenital diaphragmatic hernia. Semin Fetal Neonatal Med 19:324–330
15. Bootstaylor BS, Filly RA, Harrison MR et al (1995) Prenatal sonographic predictors of liver herniation in congenital diaphragmatic hernia. J Ultrasound Med 14:515–520
16. Plunk MR, Chapman T (2014) The fundamentals of fetal magnetic resonance imaging: part 2. Curr Probl Diagn Radiol 43(6):347–355
17. Benachi A, Cordier A, Cannie M, Jani J (2014) Advances in prenatal diagnosis of congenital diaphragmatic hernia. Semin Fetal Neonatal Med 19:331–337
18. Levine D (2001) Ultrasound versus magnetic resonance imaging in fetal evaluation. Top Magn Reson Imaging 12(1):25–38
19. Mehollin-Ray AR, Caasady CI, Cass DK, Olutoye OO (2012) Fetal MR imaging of congenital diaphragmatic hernia. Radiographics 32:1067–1084
20. Cannie M, Janis J, DeKeyyzer F et al (2009) Diffusion weighted MRI in lungs of normal fetuses and those with congenital diaphragmatic hernia. Ultrasound Obstet Gynecol 34:678–686
21. Losty PD (2014) Congenital diaphragmatic hernia: where and what is the evidence? Semin Pediatr Surg 13:278–282
22. Madenci AL, Sjogren AR, Treadwell MC et al (2013) Another dimension to survival: predicting outcomes with fetal MRI versus prenatal ultrasound in patients with congenital diaphragmatic hernia. J Pediatr Surg 48:1190–1197
23. Jeanty C, Kunisaki SM, MacKenzie TC (2014) Novel non-surgical prenatal approaches to treating congenital diaphragmatic hernia. Semin Fetal Neonatal Med 19:349–356
24. Ruano R, Lazar DA, Cass DL et al (2014) Fetal lung volume and quantification of liver herniation by magnetic resonance imaging in isolated congenital diaphragmatic hernia. Ultrasound Obstet Gynecol 43:662–669
25. Danzer E, Hedrick HL (2014) Controversies in the management of severe congenital diaphragmatic hernia. Semin Fetal Neonatal Med 19:376–384
26. Laudy JA, Van Gucht M, VanDooren MF et al (2003) Congenital diaphragmatic hernia: an evaluation of the prognostic value of the lung-to-head ratio and other prenatal parameters. Prenat Diagn 23:634–639
27. Jani JC, Peralta CF, Ruano R et al (2007) Comparison of fetal lung area to head circumference ratio with lung volume in the prediction of postnatal outcome in diaphragmatic hernia. Ultrasound Obstet Gynecol 30:850–854
28. Gorincour G, Boubenot J, Mourot MG et al (2005) Prenatal prognosis of congenital diaphragmatic hernia using MRI measurement of fetal lung volume. Ultrasound Obstet Gynecol 26:738–744
29. Rypens F, Metens T, Rocourt N et al (2001) Fetal lung volume: estimation at MR imaging – initial results. Radiology 219: 236–241
30. McHoney M (2014) Congenital diaphragmatic hernia. Early Hum Dev 90:941–946
31. Barnewolt CE, Kunisaki SM, Fauza DO et al (2007) Percent predicted lung volumes as measured on fetal MRI: a useful biometric parameter for risk stratification in congenital diaphragmatic hernia. J Pediatr Surg 42:193–197
32. Cannie M, Jani J, Chaffiotte C et al (2008) Quantification of intrathoracic liver herniation by magnetic resonance imaging and prediction of postnatal survival in fetuses with congenital diaphragmatic hernia. Ultrasound Obstet Gynecol 32:627–632
33. Lazar DA, Ruano R, Cass DL et al (2012) Defining "liver-up": does the volume of liver herniation predict outcome for fetuses with isolated left-sided congenital diaphragmatic hernia? J Pediatr Surg 47:1058–1062
34. Weidner M, Hagelstein C, Debus A et al (2014) MRI-based ratio of fetal lung volume to fetal body volume as a new prognostic marker in congenital diaphragmatic hernia. AJR Am J Roentgenol 202:1330–1336
35. Rypens F, Grignon A, Avni FE (2002) Perinatal Imaging from ultrasound to MR imaging. The Fetal Chest Grignon A, Avni FE Spinger - Verlag 2002 pp 77–012
36. Bianchi DW, Crombleholme TM, D'Alton ME, Malone FD (2010). Fetology: Diagnosis and Management of the Fetal Patient, 2nd edn by Diana Bianchi, Timothy Crombleholme McGraw Medical, New York. pp 255–306
37. Barth RA (2012) Imaging of fetal chest masses. Pediatr Radiol 42(Suppl 1):S62–S73
38. Bulas D, Egloff AM (2011) Fetal chest ultrasound and magnetic resonance imaging: recent advances and current clinical applications. Radiol Clin North Am 49:805–823

39. Epelman M, Kreiger PA, Servaes E et al (2010) The diagnosis and management of prenatally diagnosed congenital lung lesions. Semin Ultrasound CT MR 31:141
40. Daltro P, Werner H, Gasparetto TD et al (2010) Congenital chest malformations: a multimodality approach with emphasis on fetal MR imaging. Radiographics 30:385
41. Adzick NS, Harrison MR, Chrombleholme TM et al (1998) Fetal lung lesions: management and outcome. Am J Obstet Gynecol 179:884
42. Crombleholme TM, Coleman B, Hedrick H et al (2002) Cystic adenomatoid malformation volume ratio predicts outcome in prenatally diagnosed cystic adenomatoid malformation of the lung. J Pediatr Surg 37(3):331–338
43. Lecompte B, Hadden H, Coste K et al (2009) Hyperechoic congenital lung lesions in a non-selected population: from prenatal detection till perinatal management. Prenat Diagn 29:1222
44. Cavoretto P, Molina F, Poggi S et al (2008) Prenatal diagnosis and outcome of echogenic fetal lesions. Ultrasound Obstet Gynecol 32:769–783
45. Schott S, Mackensen-Haen S, Wallwiener M et al (2009) Cystic adenomatoid malformation of the lung causing hydrops fetalis: case report and review of the literature. Arch Gynecol Obstet 280:293
46. Stocker T, Dehner LP. Pediatric pathology, 2nd edn. Lippincott Williams and Wilkins, Philadelphia, PA. p 473
47. Pryce DM (1946) Lower accessory pulmonary artery with intralobar sequestration of lung: a report of seven cases. J Pathol Bacteriol 58:457
48. Hubbard AM (2001) Magnetic resonance imaging of fetal thoracic abnormalities. Top Magn Reson Imaging 12(1):18–24
49. Martin C, Darnell A, Escofet C et al (2012) Fetal MRI in the evaluation of pulmonary and digestive system pathology. Insights Imaging 3:277–293
50. Azizkhan RG, Crombleholme TM (2008) Congenital cystic lung disease: contemporary antenatal and postnatal management. Pediatr Surg Int 24:643
51. Grethel EJ, Wagner AJ, Clifton MS et al (2007) Fetal intervention for mass lesions and hydrops improves outcome: a 15-year experience. J Pediatr Surg 42:117
52. Flanagan S, Rubesova E, Hintz S et al (2013) Prenatal imaging of bronchopulmonary malformations: is there a role for late third trimester fetal MRI? Pediatr Radiol 43:205
53. Knox EM, Kilby MD, Martin WL, Khan KS (2006) In-utero pulmonary drainage in the management of primary hydrothorax and congenital cystic lung lesion: a systematic review. Ultrasound Obstet Gynecol 28:726
54. Mann S, Wilson RD, Bebbington MW et al (2007) Antenatal diagnosis and management of congenital cystic adenomatoid malformation. Semin Fetal Neonatal Med 12:477
55. Wilson RD (2008) In utero therapy for fetal thoracic abnormalities. Prenat Diagn 28:619
56. Witlox RS, Lopriore E, Walther FJ et al (2009) Single-needle laser treatment with drainage of hydrothorax in fetal bronchopulmonary sequestration with hydrops. Ultrasound Obstet Gynecol 34:355
57. Oepkes D, Devlieger R, Lopriore E, Klumpfer FJ (2007) Successful ultrasound guided laser treatment of fetal hydrops caused by pulmonary sequestration. Ultrasound Obstet Gynecol 29:457
58. Ruano R, de A Pimenta EJ, Marques da Silva M et al (2007) Percutaneous intrauterine laser ablation of the abnormal vessel in pulmonary sequestration with hydrops at 29 weeks' gestation. J Ultrasound Med 26:1235
59. Mychaliska GB, Bryner BS, Nugent C et al (2009) Giant pulmonary sequestration: the rare case requiring the EXIT procedure with resection and ECMO. Fetal Diagn Ther 25:163
60. Mallman MR, Geipel A, Bludau M et al (2014) Bronchopulmonary sequestration with massive pleural effusion: pleuroamniotic shunting vs intrafetal vascular laser ablation. Ultrasound Obstet Gynecol 44:441
61. Ruano R, da Silva MM, Salustiano EM et al (2012) Percutaneous laser ablation under ultrasound guidance for fetal hyperechogenic microcystic lung lesions with hydrops: a single center cohort and a literature review. Prenat Diagn 32:1127
62. Adzick NS (2010) Open fetal surgery for life-threatening fetal anomalies. Semin Fetal Neonatal Med 15:1
63. Olutoye OO, Coleman BG, Hubbard AM, Adzick NS (2000) Prenatal diagnosis and management of congenital lobar emphysema. J Pediatr Surg 35:792–795
64. Liu YP, Shih SL (2008) Congenital lobar emphysema: appearance on fetal MRI. Pediatr Radiol 38:1264
65. Moideen I, Nair SG, Cherian A, Rao SG (2006) Congenital lobar emphysema associated with congenital heart disease. J Cardiothorac Vasc Anesth 20(2):239–241
66. Ankermann T, Oppermann HC, Engler S et al (2004) Congenital masses of the lung, cystic adenomatoid malformation versus congenital lobar emphysema. Prenatal diagnosis and implications for postnatal treatment. J Ultrasound Med 23:1379–1384
67. Derderian SC, Trivedi S, Farrell J et al (2014) Outcomes of fetal intervention for primary hydrothorax. J Pediatr Surg 49:900–904
68. Pellegrinelli JM, Kohler A, Kohler M et al (2012) Prenatal management and thoracoamniotic shunting in primary fetal pleural effusions: a single centre experience. Prenat Diagn 32:467–471
69. Bigras JL, Ryan G, Suda K et al (2003) Echocardiographic evaluation of fetal hydrothorax: the effusion ratio as a diagnostic too. Ultrasound Obstet Gynecol 21:37–40
70. Aybard Y, Derouineau I, Aubard V et al (1998) Primary fetal hydrothorax: a literature review and proposed antenatal clinical strategy. Fetal Diagn Ther 13:325–333
71. Longaker MT, Laberge JM, Dansereau J et al (1989) Primary fetal pneumothorax: natural history and management. J Pediatr Surg 24:573–576
72. Courtier J, Poder L, Wang ZJ et al (2010) Fetal tracheolaryngeal airway obstruction: prenatal evaluation by sonography and MRI. Pediatr Radiol 40:1800–1805
73. Joshi P, Satija L, George RA et al (2012) Congenital high airway obstruction syndrome – antenatal diagnosis of a rare case of airway obstruction using multimodality imaging. Med J Armed Forces India 68:78–80
74. Martinez JM, Castañón M, Gómez O et al (2013) Evaluation of fetal vocal cords to select candidates for successful fetoscopic treatment of congenital high airway obstruction syndrome: preliminary case series. Fetal Diagn Ther 34:77–84
75. Roybal JL, Liechty KW, Hedrick HL et al (2010) Predicting severity of congenital high airway obstruction syndrome. J Pediatr Surg 45:1633–1639
76. Raman SP, Pipavath SN, Raghu G et al (2009) Imaging of thoracic lymphatic diseases. AJR Am J Roentgen 193(6):1504–1513
77. Victoria T, Andronikou S (2014) The fetal MR appearance of 'nutmeg lung': findings in 8 cases linked to pulmonary lymphangiectasia. Pediatr Radiol 44(10):1237–1242
78. Gray M, Kovatis KZ, Stuart T et al (2014) Treatment of congenital pulmonary lymphangiectasia using ethiodized oil lymphangiography. J Perinatol 34(9):720–722
79. Kayemba-Kay's S, Couvrat-Carcauzon V, Goua V et al (2014) Unilateral pulmonary agenesis: a report of four cases, Two diagnosed antenatally and literature review. Pediatr Pulmonol 49:E96–E102
80. Kuwashima S, Nishimura G, Limura F et al (2001) Low intensity fetal lungs on MRI may suggest the diagnosis of pulmonary hypoplasia. Pediatr Radiol 31:669–672
81. Kuwashima S, Kaji Y (2010) Fetal MR imaging diagnosis of pulmonary agenesis. Magn Reson Med Sci 9(3):149–152

82. Lee KA, Cho JY, Lee SM et al (2010) Prenatal diagnosis of bilateral pulmonary agenesis; a case report. Korean J Radiol 11:119–122
83. Miniati DN, Chintagumpala M, Langston C et al (2006) Prenatal presentation and outcome of children with pleuropulmonary blastoma. J Pediatr Surg 41:66–71
84. Ono K, Kikuchi A, Miyashita S et al (2007) Fetus with prenatally diagnosed posterior mediastinal lymphangioma: characteristic ultrasound and magnetic resonance imaging findings. Congential Anomalies 47:158–160
85. Goldstein I, Leibovitz Z, Noir-Nizri M (2006) Prenatal diagnosis of fetal chest lymphangioma. J Ultrasound Med 25:1437–1440
86. Takayasu H, Kitano Y, Juroda T et al (2010) Successful management of a large fetal mediastinal teratoma complicated by hydrops fetalis. J Pediatr Surg 45:E21–E24
87. Wie JH, Kim JY, Kwon JY et al (2013) Mesenchymal hamartoma of the chest wall: prenatal sonographic manifestations. J Obstet Gynaecol Res 39(6):1217–1221
88. Martinez-Varea A, Vila-Vives JM, Hidalgo-Mora JJ et al (2012) Case report: mesenchymal hamartoma: prenatal and postnatal diagnosis by imaging. Case Rep Obstet Gynecol 2012:954241
89. Calvo-Garcia MA, Lim FY, Stanek J et al (2014) Congenital peribronchial myofibroblastic tumor: prenatal imaging clues to differentiate from other fetal chest lesions. Pediatr Radiol 44:479–483
90. Victoria T, Capilla E, Chauvin NA et al (2011) MR evaluation of fetal demise. Pediatr Radiol 41:884–889